Journal of Computational and Applied Mathematics 45 (1993) 357–365
North-Holland
CAM 1355

Letter Section

Convergence behaviour of defect correction for hyperbolic equations

P.W. Hemker

Centrum voor Wiskunde en Informatica, Amsterdam, Netherlands

J.-A. Désidéri

Institut National de Recherche en Informatique et en Automatique (INRIA), Centre de Sophia Antipolis, Valbonne, France

Received 12 October 1992

Abstract

Hemker, P.W. and J.-A. Désidéri, Convergence behaviour of defect correction for hyperbolic equations, Journal of Computational and Applied Mathematics 45 (1993) 357–365.

In this note we present results about the convergence rate of a defect correction process for the solution of second-order accurate convection problems. The operator to be inverted is a stable, first-order accurate discretisation. It is shown how the choice of the second-order discretisation scheme influences the convergence rate. Neither the second-order upwind, nor the central scheme converge, but intermediate schemes do.

Keywords: Defect correction; hyperbolic problems; convection problems; Euler equations.

1. Introduction

The nonlinear multigrid method is an efficient method for the solution of the compressible Navier–Stokes equations with a large Reynolds number, or for the Euler equations [5,6]. The relaxation procedure being the workhorse of the multigrid method, the existence of a relaxation routine suited for fast reduction of the high-frequency error components in the solution of the discrete equations is essential for this success [5]. A good relaxation routine is found in point-

Correspondence to: Prof. P.W. Hemker, Afdeling Numerieke Wiskunde, Centrum voor Wiskunde en Informatica, P.O. Box 4079, 1009 AB Amsterdam, Netherlands. e-mail: pieth@cwi.nl.

or linewise nonlinear (collective) Gauss–Seidel relaxation, assumed that we solve the first-order accurate discrete equations.

For the second-order discretisation the relaxation procedures are significantly less efficient. This is the reason why an additional iteration procedure is introduced as an outer loop: iterative defect correction (ItDeC [1]). The second-order accurate approximation is now computed by the iteration

$$N_h^1(q_h^{(1)}) = 0, \tag{1}$$

$$N_h^1(q_h^{(i+1)}) = N_h^1(q_h^{(i)}) - N_h^2(q_h^{(i)}), \quad i = 1,2,\ldots. \tag{2}$$

Here N_h^1 and N_h^2 denote the first- and second-order (nonlinear) discrete operators. Only systems for first-order accurate discrete equations are solved, but the fixed point of the iteration is the solution of the second-order discrete system

$$N_h^2(q_h) = 0. \tag{3}$$

For the approximate solution of each iterate $q_h^{(i+1)}$, $i = 0,1,\ldots$, a small number of multigrid iteration steps (and in many cases only a single step) is sufficient.

It is a classical result that, under easily satisfied conditions, the second iterate $q_h^{(2)}$ is already second-order accurate [4, Section 14.2.2]. This result describes the convergence behaviour for the low-frequency difference between the first- and second-order discrete approximations. It explains why the convergence is fast for smooth solutions and fine grids. However, for the Navier–Stokes equations with high Reynolds number and for the Euler equations, sharp layers or discontinuities may exist in the solution. Therefore, it is of interest to study the convergence behaviour for defect correction also for high-frequency components in the error (i.e., in the difference between the first- and the second-order discretisation).

2. Linear model problem

In this note we restrict ourselves to the Euler equations. These equations form a hyperbolic system of conservation laws. To analyse the convergence for these equations, we first study the linear model problem in two dimensions

$$\frac{\partial}{\partial t}q + a\frac{\partial q}{\partial x} + b\frac{\partial q}{\partial y} = 0. \tag{4}$$

Although we are mainly interested in the steady state, we consider here the time-dependent problem in order to introduce a "flow direction" so that inflow and outflow boundaries can be identified. The vector $(a,b)^T$ determines the flow direction, and with $a > 0$ the flow is in the positive x-direction.

For the first-order discretisation, the simple upwind scheme is used. This scheme is described by its stencil

$$L_h^1 \sim \begin{bmatrix} & 0 & \\ -a & a+b & 0 \\ & -b & \end{bmatrix}. \tag{5}$$

For the second-order discretisation, various alternatives are available. Obvious possibilities are the central scheme and the second-order upwind scheme, with the stencils

$$L_h^{2C} \sim \begin{bmatrix} & \frac{1}{2}b & \\ -\frac{1}{2}a & 0 & \frac{1}{2}a \\ & -\frac{1}{2}b & \end{bmatrix} \quad \text{and} \quad L_h^{2U} \sim \begin{bmatrix} & & 0 & & \\ & & 0 & & \\ \frac{1}{2}a & -2a & \frac{3}{2}(a+b) & 0 & 0 \\ & & -2b & & \\ & & \frac{1}{2}b & & \end{bmatrix}. \tag{6}$$

The corresponding linear operators are denoted by L_h^1, L_h^{2C} and L_h^{2U}, for the first-order and the second-order central and upwind scheme respectively. By linear combination of L_h^{2C} and L_h^{2U} a scale of second-order schemes is obtained, the so-called κ-schemes

$$L_h^{2\kappa} = \tfrac{1}{2}(1+\kappa)L_h^{2C} + \tfrac{1}{2}(1-\kappa)L_h^{2U}. \tag{7}$$

Here $\kappa \in [-1,1]$ is a free parameter that determines the particular scheme; $\kappa = 0$ corresponds with Fromm's scheme. Being interested in the convergence of ItDeC, we study the amplification operator of the error

$$M_h^\kappa = (L_h^1)^{-1}(L_h^1 - L_h^{2\kappa}). \tag{8}$$

3. One-dimensional analysis

We first study the operator M_h^κ in the one-dimensional case. Then, without loss of generality, we have

$$L_h^1 \sim [-1, 1, 0] \tag{9}$$

and

$$L_h^{2\kappa} \sim \tfrac{1}{4}(1+\kappa)[-1,0,1] + \tfrac{1}{4}(1-\kappa)[1,-4,3,0,0]. \tag{10}$$

For an infinite, regular grid with mesh width h, eigenfunctions for these operators are u_ω, $\omega \in [-\pi/h, \pi/h]$, where $u_\omega(jh) = e^{i\omega hj}$. Corresponding eigenvalues of the operator M_h^κ are

$$\widehat{M}_h^\kappa(\omega) = i \sin(\tfrac{1}{2}\omega h)\cos(\tfrac{1}{2}\omega h) + \kappa \sin^2(\tfrac{1}{2}\omega h). \tag{11}$$

This shows that the eigenvalues are located in the complex plane on an ellipse with axes $x \in [0, \kappa]$, $y \in [-\frac{1}{2}, \frac{1}{2}]$. From (11) we see that the upper bound for the convergence factor is

$$\sup_{\omega \in [-\pi/h, \pi/h]} |\widehat{M}_h^\kappa(\omega)| = \sup_{t \in [0,1]} \sqrt{\kappa^2 t^2 + t(1-t)}.$$

Thus, as upper bounds we find

$$\sup_{\omega \in [-\pi/h, \pi/h]} |\widehat{M}_h^\kappa(\omega)| = \frac{1}{2}\frac{1}{\sqrt{1-\kappa^2}}, \quad \text{for } \kappa^2 \leqslant \tfrac{1}{2}, \tag{12}$$

and

$$\sup_{\omega\in[-\pi/h,\pi/h]} |\widehat{M}_h^{\kappa}(\omega)| = |\kappa|, \quad \text{for } \tfrac{1}{2} \leqslant \kappa^2 \leqslant 1. \tag{13}$$

These expressions describe the convergence if no boundaries are present in the domain. To obtain an impression of the influence of the inflow Dirichlet boundary, we consider grid functions on a uniform partition $\{x_i = ih; i = 0, 1, 2, \ldots\}$ of the half-line $[0, \infty)$ and we restrict ourselves to error components that vanish for large x_i. The operators L_h^1 and $L_h^{2\kappa}$ are again described by (9), (10), except for the first two equations in the system, which are determined by the boundary discretisation.

The eigenfunctions u_λ of M_h^{κ} and the corresponding eigenvalues λ satisfy the relation $L_h^{2\kappa} u_\lambda = (1-\lambda) L_h^1 u_\lambda$, and from (10) it follows that u_λ has the form $u_\lambda(jh) = A_0 + A_1\mu_1^j + A_2\mu_2^j$, where μ_1 and μ_2 are roots of the equation

$$\tfrac{1}{2}(1+\kappa)\mu^2 + (2\lambda - \kappa)\mu - \tfrac{1}{2}(1-\kappa) = 0.$$

A straightforward computation [3] shows

$$\lambda = \tfrac{1}{2}(\kappa \pm \mathrm{i}\sqrt{1-\kappa^2}\cos\theta), \quad \theta \neq 0 \bmod \pi. \tag{14}$$

This shows that all eigenvalues are located on a line segment in the complex plane at a distance $\frac{1}{2}\kappa$ from the imaginary axis and that all eigenvalues satisfy $|\lambda| \leqslant \frac{1}{2}$ (see Fig. 1).

In the case $\kappa = \pm 1$, we still have $\rho = \max|\lambda| = \frac{1}{2}$, but the eigenvalues coalesce and the eigenvectors are no longer independent. Consequently, in the operator decomposition Jordan blocks J arise. In the one-dimensional case, on a finite interval, the size of these blocks is $N-1$, where N is the number of mesh points. Then the convergence behaviour after n iterations of ItDeC is described by $\tau_n = \|J^n\|_\infty$, where

$$J^n = \begin{pmatrix} \rho^n & & & \\ \xi_j^n & \rho^n & & \\ \vdots & \ddots & \ddots & \\ & & \xi_j^n & \rho^n \end{pmatrix}, \quad \text{with } \xi_j^n = \binom{n}{j}\rho^{n-j}.$$

It follows that $\tau_n \geqslant \max_{j=0,1,2,\ldots,N}|\xi_j^n|$, and hence

- it is possible that $\tau \geqslant 1$ if $n < N$;
- $\tau_n \approx n^{N-1}\rho^n$ for $n \to \infty$, and hence the asymptotic convergence rate of the iteration is $\rho \log|n|$;
- the sequence $\{\tau_\nu\}_{\nu\leqslant n}$ is guaranteed to be decreasing only for $n > N/(1-\rho)$. In our case $\rho = \frac{1}{2}$. This implies that the iteration may show no convergence for the first $2N$ iteration steps.

These phenomena are seen in practice indeed, as is shown in Figs. 2(a)–2(d).

If $\kappa \neq \pm 1$ but $1 \leqslant |\kappa| \leqslant \frac{1}{2}\sqrt{2}$, the convergence during the first $2N$ iteration steps is dominated by the behaviour as described by the Fourier analysis (13), i.e., a convergence rate of $|\kappa|$ is seen. For all $\kappa \in [-1, +1]$ the convergence rate has the lower bound $\rho = \frac{1}{2}$.

In summary, for the one-dimensional problem we distinguish different phases in the convergence of the iterated defect correction. In most cases we first observe an impulsive start, where all components corresponding with small eigenvalues are damped. For the regular schemes (i.e., $|\kappa|$ different from 1) soon an asymptotic rate of $\frac{1}{2}$ is obtained. For the (near-)pathological cases (i.e., $|\kappa|$ close to 1), after the impulsive start, we distinguish first a Fourier (or pseudo-convection) phase

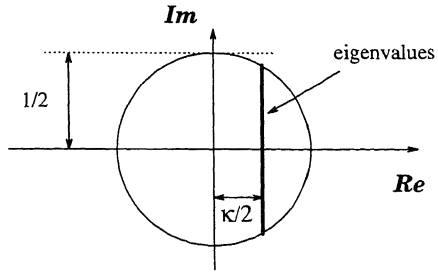

One dimensional situation

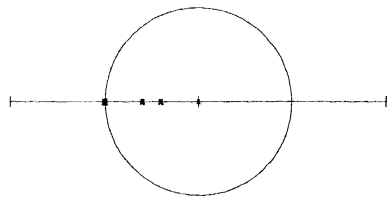

Two dimensional situation, $\kappa = -1$

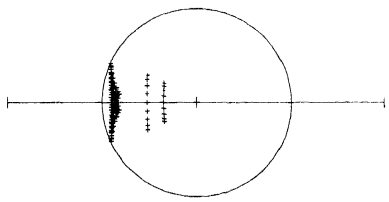

Two dimensional situation, $\kappa = -0.9$

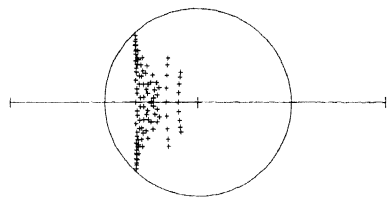

Two dimensional situation, $\kappa = -2/3$

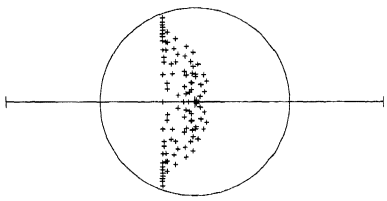

Two dimensional situation, $\kappa = -1/3$

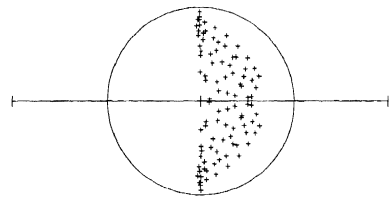

Two dimensional situation, $\kappa = 0$

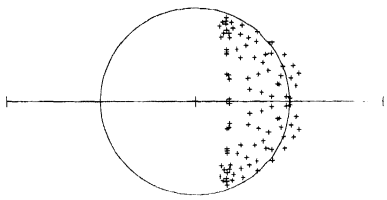

Two dimensional situation, $\kappa = 1/3$

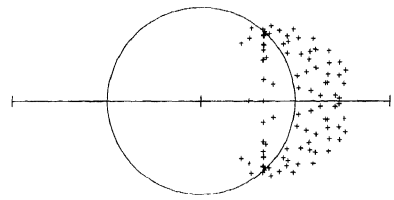

Two dimensional situation, $\kappa = 2/3$

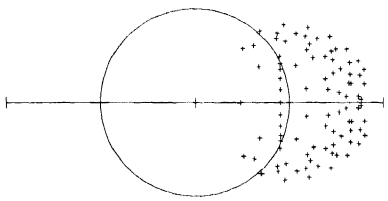

Two dimensional situation, $\kappa = 0.9$

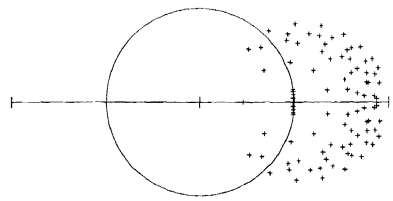

Two dimensional situation, $\kappa = 0.99$

Fig. 1. Location of the eigenvalues of the amplification matrix M_h^κ in the complex plane, relatively to the circle of radius $\frac{1}{2}$, for the one- and the two-dimensional model problem. Except for the first one-dimensional figure, the mesh is 10×10 and the ratio $a/b = 2/3$.

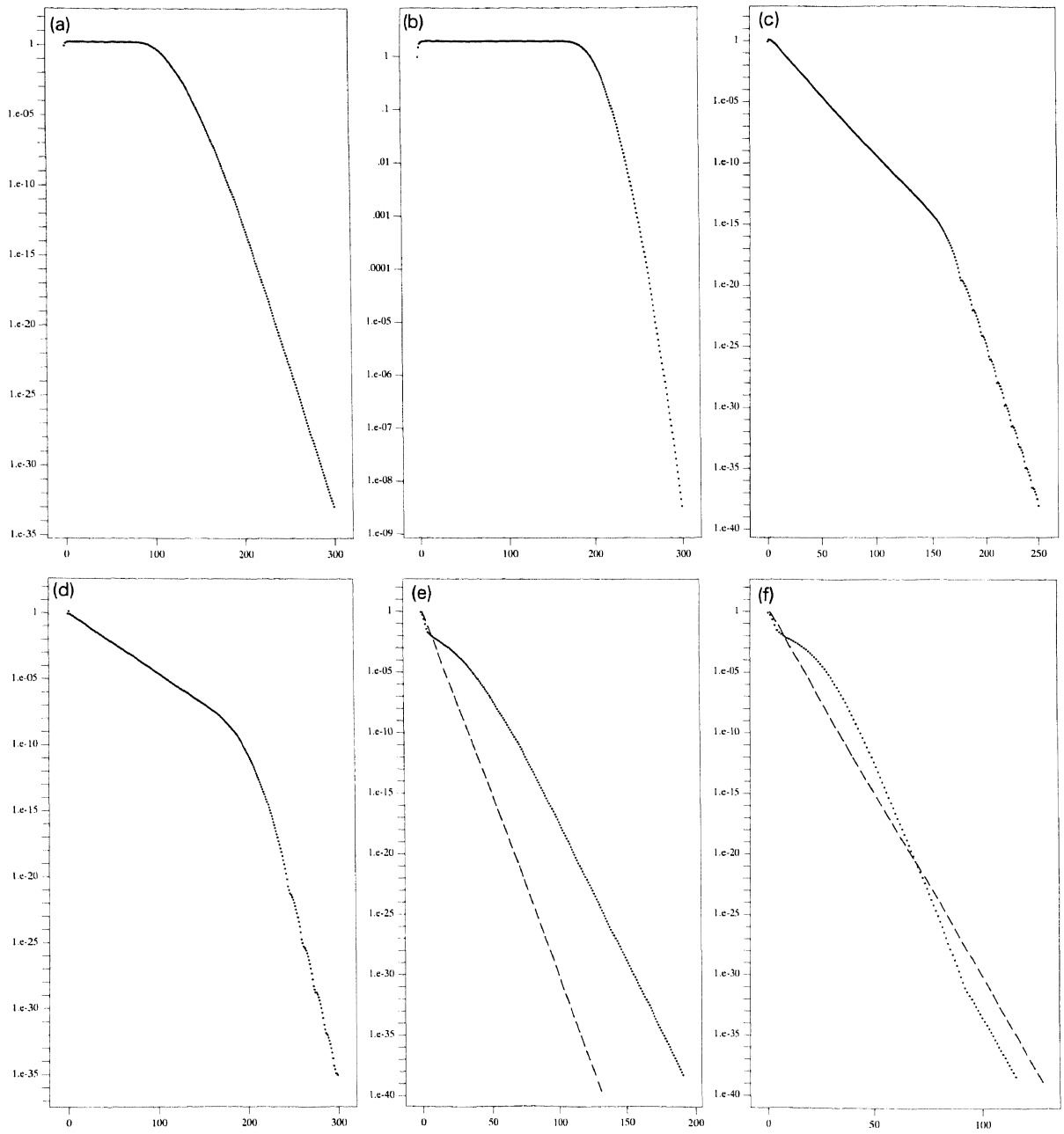

Fig. 2. Convergence of ItDeC for the one- or two-dimensional linear test problem. The sup-norm of the error is plotted against the number of iterations. The dashed line corresponds with a convergence rate $\rho = \frac{1}{2}$. (a) One-dimensional, $N = 50$, $\kappa = 1$; (b) one-dimensional, $N = 100$, $\kappa = 1$; (c) one-dimensional, $N = 100$, $\kappa = 0.8$; (d) one-dimensional, $N = 100$, $\kappa = -0.9$; (e) two-dimensional, 40×40 mesh, $\kappa = \frac{1}{3}$; (f) two-dimensional, 40×40 mesh, $\kappa = 0$.

for about $2N$ iterations, in which the convergence is described by the Fourier analysis. After $2N$ iterations the asymptotic rate $\frac{1}{2}$ is found. In the truly degenerate cases ($|\kappa| = 1$) we recognise a Fourier (pseudo-convection) phase, where the error does not decrease for $2N$ iterations, and the logarithmic asymptotic rate due to the large Jordan block in the eigenvalue decomposition.

4. Two-dimensional analysis

In principle, the Fourier analysis for the two-dimensional difference operators (5), (6) is completely analogous to the one-dimensional case. With the Fourier modes defined by $u_\omega(hj) = e^{i(\omega_1 h_1 j_1 + \omega_2 h_2 j_2)}$, where the subscripts refer to the x- and the y-directions respectively, we find

$$\hat{L}_h^1(\omega) = 2ia e^{-i\omega_1 h_1/2} \sin(\tfrac{1}{2}\omega_1 h_1) + 2ib e^{-i\omega_2 h_2/2} \sin(\tfrac{1}{2}\omega_2 h_2) \tag{15}$$

and

$$\begin{aligned} \hat{L}_h^{2\kappa}(\omega) = {} & 2ia e^{-i\omega_1 h_1/2} S_1 (C_1^2 + iS_1 C_1 + (1-\kappa) S_1^2) \\ & + 2ib e^{-i\omega_2 h_2/2} S_2 (C_2^2 + iS_2 C_2 + (1-\kappa) S_2^2), \end{aligned} \tag{16}$$

where $S_1 = \sin(\frac{1}{2}\omega_1 h_1)$, $S_2 = \sin(\frac{1}{2}\omega_2 h_2)$, $C_1 = \cos(\frac{1}{2}\omega_1 h_1)$ and $C_2 = \cos(\frac{1}{2}\omega_2 h_2)$.

As the amplification factor we find

$$\begin{aligned} g(\omega) = {} & \left\| \hat{M}_h^\kappa(\omega) \right\| = \left\| (\hat{L}_h^1)^{-1} (\hat{L}_h^1 - \hat{L}_h^{2\kappa}) \right\| \\ = {} & \Big\{ (a_1 S_1^2 (1 - (1-\kappa) S_1^2) + a_2 S_2^2 (1 - (1-\kappa) S_2^2))^2 \\ & + (1-\kappa)^2 (a_1 S_1^3 C_1 + a_2 S_2^3 C_2)^2 \Big\}^{1/2} \\ & \times \Big\{ (a_1 S_1^2 + a_2 S_2^2)^2 + (a_1 S_1 C_1 + a_2 S_2 C_2)^2 \Big\}^{-1/2}. \end{aligned} \tag{17}$$

This expression can be used to determine the convergence rate for the separate modes on an infinite domain. It shows that, for a given κ, we can never expect a better convergence rate in the two-dimensional case than in the one-dimensional case.

For the analysis of the two-dimensional case on a finite domain, we refer to [2,3]. Essentially, the results for two space dimensions can be seen as a perturbation of the results for one dimension. Analogous to the one-dimensional domain, the location of the eigenvalues is shown in Fig. 1. We now find the eigenvalues not on a line segment in the complex plane, but in a cloud near that line segment. The real part of the eigenvalues is generally larger than is the case in one dimension (for the same κ). This means that the cloud is shifted to the right of the corresponding line segment. For the case of large κ ($\kappa \approx +1$), the cloud is larger than for small κ ($\kappa \approx -1$).

For different values of κ and for different values of N the location of the eigenvalues in the complex plane is shown in Fig. 1. In this figure the ratio a/b is 2/3. In [3] one finds similar results for $a/b = 1/1$ or $a/b = 1/100$.

In Fig. 2 the convergence behaviour is shown for the model problem on a 40×40 mesh. For $\kappa \leqslant 0$, the cloud of eigenvalues is still contained in the circle $|z| \leqslant 0.5$, so $\rho(M_h^\kappa) \leqslant 0.5$ if $\kappa \leqslant 0$. However, for $0 < \kappa \leqslant 1$ we find possibly $\rho(M_h^\kappa) > 0.5$, and for large κ we have $\lim_{\kappa \to +1} \lim_{h \to 0} \rho(M_h^\kappa) = 1$. This explains why a convergence rate $\rho(M_h^\kappa) > 0.5$ is found for $\kappa = \frac{1}{3}$ in Fig. 2, whereas $\rho(M_h^\kappa) = 0.5$ for $\kappa = 0$. For more details we refer to [3].

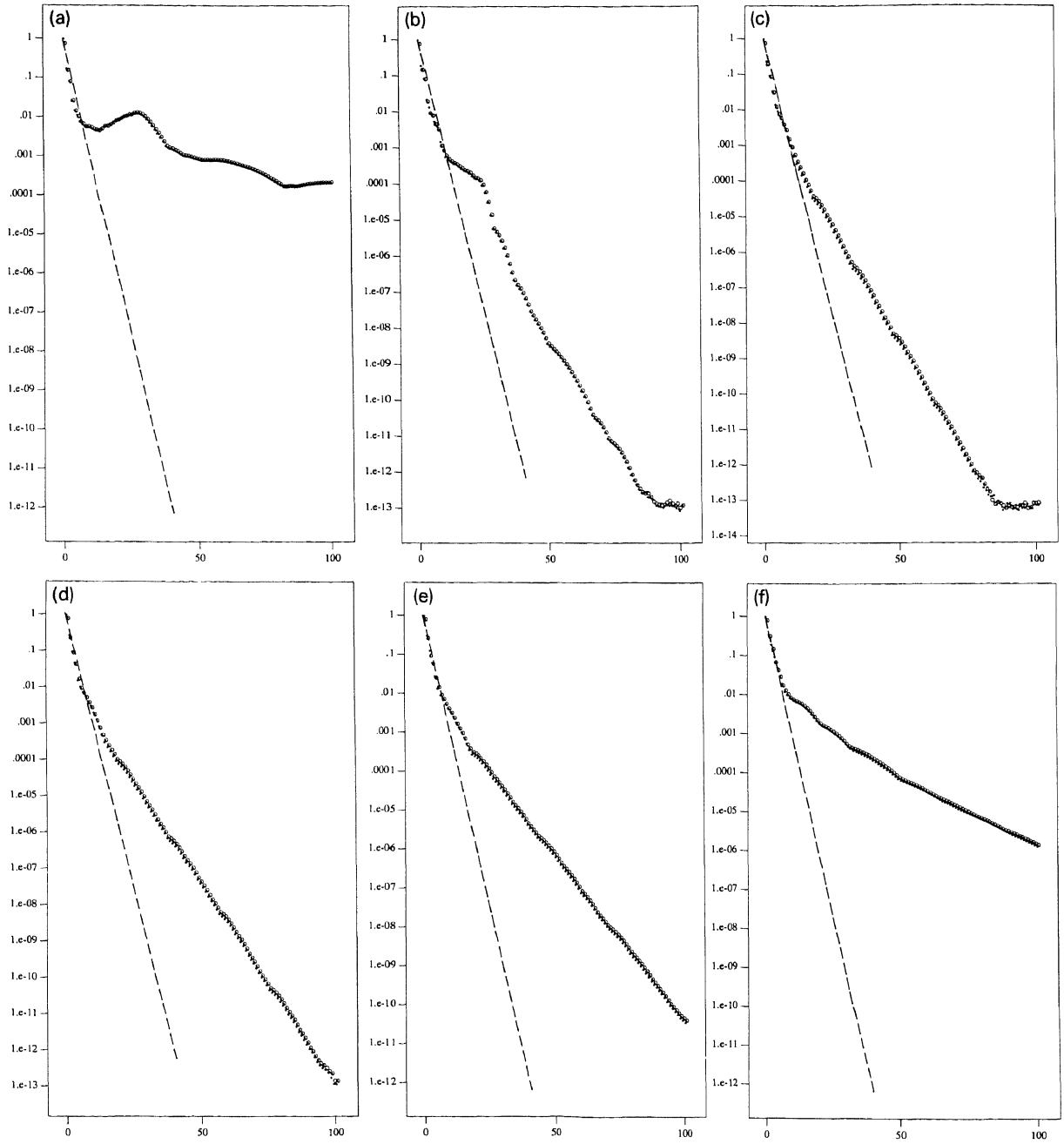

Fig. 3. Convergence of ItDeC for the Euler equations with contact discontinuity. The sup-norm of the error is plotted against the number of iterations. The dashed line corresponds with a convergence rate $\rho = \frac{1}{2}$.
(a) $\kappa = -1$; (b) $\kappa = -0.8$; (c) $\kappa = -\frac{1}{3}$; (d) $\kappa = 0$; (e) $\kappa = \frac{1}{3}$; (f) $\kappa = 0.8$.

5. Euler equations

A similar behaviour, dependent on κ, as for the linear model problem, is found for the nonlinear Euler equations. In Fig. 3 we show the convergence behaviour for a problem that describes an Euler flow with a pure contact discontinuity on a square $[0,1] \times [0,1]$. The boundary conditions are specified so that the contact discontinuity exists along the line $x = y$. The flow is from bottom-left to top-right and the boundary conditions are: at left (inflow) $u = v = 0.5$, $c = \sqrt{2}$; at bottom (inflow) $u = v = 1.0$, $c = \sqrt{2}$; at outflow (right, and top) $p = 1.0$ (p: pressure; c: speed of sound; u, v: velocity components).

The first-order discrete equations are solved by a nonlinear multigrid method [5]. It employs a nonlinear symmetric point-Gauss–Seidel relaxation as a smoother and a nested sequence of Galerkin discretisations for the coarse grid corrections. Experience has shown that a small number of iteration cycles of this multigrid method solves the discrete system to a high degree of accuracy. In the experiments shown, three FAS V-cycles were applied for each single defect correction step. It was shown by experiments that the same results were obtained for multigrid iteration with two through five FAS V-cycles. All initial estimates were obtained by interpolation from a first-order accurate solution on a coarser grid.

For this flow with a contact discontinuity, $\kappa = 1$ gives a diverging process (not shown), and $\kappa = 0.8$ shows worse convergence than $\kappa = -0.8$. The asymmetry in the convergence behaviour with respect to $\kappa > 0$ (worse) and $\kappa < 0$ (better convergence) might be understood by the location of the eigenvalues in the complex plane (as shown in Fig. 1). There we see that more eigenvalues are located in the neighbourhood of the origin for $\kappa < 0$ than for $\kappa > 0$. This may be of greater importance for the nonlinear equations, where the corresponding eigenvectors are excited again and again, than for the linear problems, where the effect of these eigenvalues is no longer seen after a sufficient number of iterations.

References

[1] K. Böhmer, P. Hemker and H. Stetter, The defect correction approach, *Comput. Suppl.* **5** (1984) 1–32.
[2] J.-A. Désidéri, Preliminary results on the iterative convergence of a class of implicit schemes, Report No. 490, INRIA, 1986.
[3] J.-A. Désidéri and P. Hemker, Analysis of the convergence of iterative implicit and defect correction algorithms for hyperbolic problems, Report No. 1200, INRIA, 1990.
[4] W. Hackbusch, *Multigrid Methods and Applications* (Springer, Berlin, 1985).
[5] P.W. Hemker and S.P. Spekreijse, Multiple grid and Osher's scheme for the efficient solution of the steady Euler equations, *Appl. Numer. Math.* **2** (6) (1986) 475–493.
[6] B. Koren, Multigrid and defect correction for the steady Navier–Stokes equations, application to aerodynamics, Centrum voor Wiskunde en Informatica, Amsterdam, 1990.